Description of the Gamow-Teller resonance within the phonon damping model

Nguyen Dinh Dang,[1,*] Toshio Suzuki,[2] and Akito Arima[1,3]
[1]*RI-beam Factory Project Office, RIKEN, 2-1 Hirosawa, Wako, Saitama 351-0198, Japan*
[2]*Department of Physics, College of Humanities and Sciences, Nihon University, Sakurajosui 3-25-40, Setagaya-ku, Tokyo 156-8550, Japan*
[3]*House of Councillors, Nagata-cho 2-1-1, Chiyoda-ku, Tokyo 100-8962, Japan*
(Received 26 November 2000; revised manuscript received 25 April 2001; published 5 July 2001)

The phonon damping model is extended to describe the damping of charge-exchange resonances. The formalism is applied to calculate the strength distribution of the Gamow-Teller resonance in ^{90}Nb. The results obtained are found to be in reasonable agreement with recent experimental data and with those of a previous study with explicit microscopic coupling to $2p2h$ configurations using a realistic interaction.

DOI: 10.1103/PhysRevC.64.027303 PACS number(s): 24.30.Cz, 25.40.Kv, 27.60.+j

The Gamow-Teller resonance (GTR) is a charge-exchange resonance as it is caused by exchanging neutrons with protons in a nucleus. The total transition strength of the GTR is given by the model-independent sum rule (SR) $S_{\beta_-}-S_{\beta_+}=3(N-Z)$, which should be nearly exhausted by the β_- transition strength summed over all Gamow-Teller (GT) states in the daughter nucleus $(Z+1,N-1)$ formed after the (p,n) reactions. The quenching of GTR had been a problem addressed to the missing of GTR strength for many years as the GTR had been observed only with about 60% of the GTR SR for many nuclei all over the periodic table [1]. Two physically different mechanisms have been brought forward to resolve the problem of GTR quenching. The first mechanism (A) [2–6], which considers only structureless nucleons, suggests that the coupling of the GTR state to more complicated configurations such as $2p2h$, using a microscopic interaction such as those derived from a G matrix with a Reid soft-core potential (the M3Y interaction) [4,6] or Bonn potential (the HM3A version) [5], spreads the GTR strength to the region of high excitation energies E. This leads to a high-lying tail of GTR, which extends up to $E\simeq 50$–60 MeV. Until very recently, it was experimentally impossible to extract this continuous and structureless tail from the background. This explains why only about half of the GTR was experimentally seen. The second mechanism (B) [7], which involves subnucleonic degrees of freedom, proposes that the $\Delta(1232)$-isobar–neutron-hole admixture in the wave function attracts a substantial part of the GTR strength to the region of Δ-hole states at around 300 MeV of excitation energy, causing a quenching of the GTR strength in the low-energy region. In 1997, Wakasa *et al.* [8] succeeded to extract the high-lying tail of GTR, which extends up to 50 MeV in the excitation energy of the daughter nucleus ^{90}Nb formed after the reaction ^{90}Zr$(p,n)^{90}$Nb. This result confirms the validity of mechanism (A) above, leaving little room for mechanism (B). The experimental data of [8] are supported by the results of several theoretical studies, which treat the coupling of one-particle–one-hole $(1p1h)$ GT states with $2p2h$ configurations in a microscopic manner [4–6].

Recently, the phonon damping model (PDM) has been proposed to study the damping of the giant dipole resonance (GDR) in highly excited nuclei [9,10]. The PDM later was applied to study multiple phonon resonances such as double GDR [11] in stable nuclei as well as the pygmy dipole resonance in neutron-rich nuclei [12]. The PDM treats the damping of a giant resonance (GR) as the result of coupling of the GR phonon to many noncollective ph configurations (at zero temperature T), while at $T\neq 0$ couplings to pp and hh configurations are also taken into account. This mechanism (at $T=0$) has been shown to be effectively equivalent to mechanism (A) mentioned above [6]. The aim of the present paper is to test the validity of the PDM in a further development of this model, namely, its extension to the study of charge-exchange resonances.

Within the PDM the propagation of the phonon excitation, which generates the GR, is described by the Green's function $G_q(E)$:

$$G_q(E)=\frac{1}{2\pi}\frac{1}{E-\omega_q-P_q(E)}. \tag{1}$$

The GR spreading width $\Gamma_{\rm GR}$ located at energy $\omega=\omega_{\rm GR}$ is defined via the imaginary part of the analytic continuation of the polarization operator $P_q(E)$ into the complex energy plane $E=\omega\pm i\varepsilon$ as

$$\Gamma_{\rm GR}=2\gamma_q(\omega)\big|_{\omega=\omega_{\rm GR}}=2\big|{\rm Im}P_q(\omega\pm i\varepsilon)\big|_{\omega=\omega_{\rm GDR}}. \tag{2}$$

The GR energy $\omega_{\rm GR}$ is defined as the solution $\bar{\omega}$ of the following equation for the pole of the Green's function in Eq. (1):

$$\omega-\omega_q-P_q(\omega)=0, \tag{3}$$

where $P_q(\omega)$ (ω is real) is the real part of $P_q(E)$. The explicit expression of the polarization operator $P_q(E)$ depends on the version of the PDM. Within the PDM-1, the polarization operator is defined by Eq. (2.26) of [9] (superfluid pairing not included) or Eq. (14) of [12] (pairing included). The damping $\gamma_q(\omega)$ is given explicitly by Eqs. (2.28) of [9] or

*On leave of absence from the Institute of Nuclear Science and Technique, VAEC, Hanoi, Vietnam. Electronic address: dang@rikaxp.riken.go.jp

(15) of [12], respectively. Within the PDM-2, the polarization operator $P_q(E)$ has a more complicated form given by Eq. (2.17) in [10] (pairing not included), while the GR width is calculated using Eq. (2). The PDM-1 includes the coupling of the phonon operator only to the lowest-order graphs in the vertex expansion, which correspond to ph (at $T=0$) as well as pp and hh (at $T\neq 0$) configurations, while the effects of higher-order graphs are effectively taken into account by adjusting the parameter $F_1=F_{ph}^{(q)}$ of the ph-phonon coupling (at zero temperature). The PDM-2 explicitly takes into account the coupling to "$1p1h\otimes$ phonon" configurations in the denominator of the polarization operator $P_q(E)$, which is most responsible for the GR spreading (at $T=0$). Because of this, the parameter F_1 should be renormalized within the PDM-2 to a much smaller value (about one order of magnitude or more) so that both versions produce similar results (compare Tables I in [9,10]). The PDM has been applied so far to study $E1$ resonances. The essential step in extending this model to the study of charge-exchange resonances is to consider the coupling of GR phonons to only proton- (π-) particle–neutron- (ν-) hole states, which correspond to a β_- transition. This is tantamount to the summation over only $(ss')=(p_\pi,h_\nu)$ [or $(jj')=(p_\pi,h_\nu)$ in [12]] in the equations for $P_q(E)$ and $\gamma_q(E)$ mentioned above. The GR strength function $S_{\rm GR}(\omega)$ is calculated using the analytic properties of the Green's function (1) as [9]

$$S_{\rm GR}(\omega)=\frac{1}{\pi}\,\frac{\gamma_{\rm GR}(\omega)}{(\omega-\overline{\omega})^2+\gamma_{\rm GR}^2(\omega)}. \tag{4}$$

For GTR, the integrated strength, or the non-energy-weighted sum of strength (NEWSS), $\mathcal{S}$ is normalized to the GTR SR as

$$\mathcal{S}\equiv C_{\rm GT}\int_0^{E_{\rm max}} S_{\rm GR}(\omega)\,d\omega=3(N-Z), \tag{5}$$

with the normalization factor $C_{\rm GT}$, neglecting a small contribution of the β_+ process. This factor takes the contribution of the GT-transition operator effectively into account.

We calculated the β_- strength distribution in ^{90}Nb formed after the ^{90}Zr$(p,n)^{90}$Nb reaction. The single-particle energies of ^{90}Zr are obtained within the Hartree-Fock method using the SGII interaction [13]. The δ function in Eq. (2) is smoothed using the representation $\delta(x)=[(x-i\varepsilon)^{-1}-(x+i\varepsilon)^{-1}]/(2\pi i)$ with $\varepsilon=0.3$ MeV. We follow the same procedure of selecting the PDM parameters described in detail in [9,10,12]. According to it, the unperturbed phonon energy ω_q in Eqs. (1) and (3) and the ph-phonon coupling vertex $F_1\equiv F_{p_\pi h_\nu}^{(q)}$ for all (p_π,h_ν) are chosen so that the GTR width, calculated from Eq. (2), and the GTR energy, found as the solution of Eq. (3), reproduce their corresponding experimental values. As no experimental value for the spreading width of the total GTR strength distribution is available, the first criterion of the parameter selection is replaced with reproducing the overall GTR line shape in the region of the GTR peak. A proton pairing gap $\Delta_\pi=1.3$ MeV is included in the PDM-1 following [12].

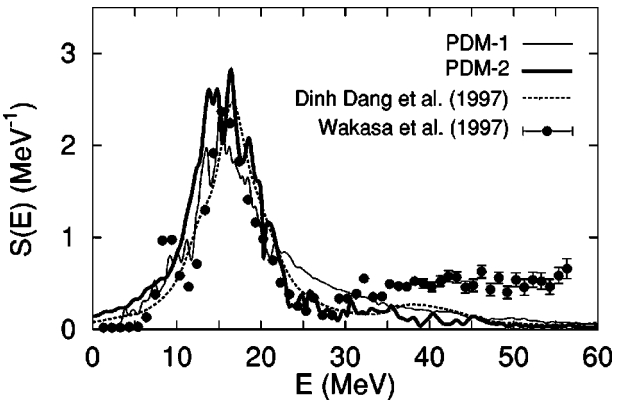

FIG. 1. Strength function of the GTR for ^{90}Nb. Excitation energies E are measured with respect to the ground state of ^{90}Zr. The thin and thick solid lines are the results obtained within the PDM-1 and PDM-2, respectively. The dotted line represents the result of the microscopic calculations of Ref. [6] using a smearing parameter of 2 MeV. The data points are the experimental results of Ref. [8].

Within the PDM-2, in order to simulate the coupling of GTR to several intermediate collective phonons in the "$1p1h\oplus$ phonon" and two-phonon configurations, we allow the energy $\omega_{q'}$ in Eqs. (2.17) and (2.18) of [10] to take six values from 5 to 30 MeV in steps of 5 MeV. This procedure yields the following values for the PDM parameters: $\omega_1=15.5$ MeV and $F_1=0.9874$ (within the PDM-1) or $F_1=7.6\times10^{-2}$ MeV (within the PDM-2) for all phonon multipolarities. An inclusion of more intermediate phonons leads to a renormalization of F_1 to obtain a similar result within the PDM-2. The strict restriction of an explicit inclusion of coupling to only "$1p1h\otimes$ phonon" configurations within the PDM-2 does not allow adjusting the parameter F_1 to take into account effects beyond that. Therefore, calculations within the PDM-2 still have to use an additional smearing parameter $\Delta\gamma=1$ MeV to account for the contribution of higher-order graphs as well as the escape width due to the coupling to the continuum, which are not explicitly included in the PDM-2 (see [10] and also [5]).

Shown in Fig. 1 is the normalized strength function $S(E)\equiv C_{\rm GT}S_{\rm GT}(E)$ of GTR for ^{90}Nb, calculated within the PDM-1 (thin solid line) and PDM-2 (thick solid line). They are plotted as a function of excitation energy E, which is measured from the ground state of ^{90}Zr. The normalization factor $C_{\rm GT}$ is 35.65, using which we get NEWSS $=3(N-Z)=30$ at $E_{\rm max}=70$ MeV. The experimental strength distribution from [8] (data points) and the result of microscopic calculations of [6] with coupling to $2p2h$ states via two-phonon configurations (dotted curve), whose structure is defined within the random-phase approximation, are also shown for comparison. This figure shows that the theoretical predictions agree fairly well with the data within the region of the GTR peak up to $E\simeq 22$–25 MeV. In the region beyond the GTR ($E>25$ MeV), the tail obtained within the PDM-1 is more enhanced than the one of microscopic calculations in [6] up to 35 MeV. At the same time the PDM-2 produces less strength in the high-lying tail than the PDM-1. We also carried out a test calculation without pairing within the PDM-1. This shifts up the GTR peak by around 1.5 MeV.

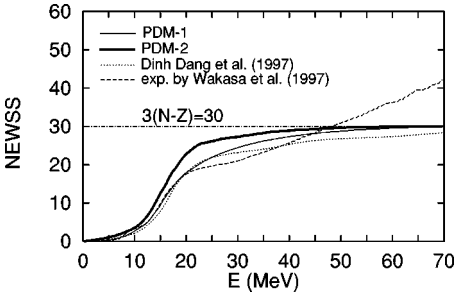

FIG. 2. NEWSS for GTR in ^{90}Nb as a function of $E_{\max}$. The dashed line is the experimental result of Ref. [8]. The notation for thin and thick solid lines is as in Fig. 1.

The strength between 16 and 22 MeV increases slightly. The high-lying tail remains nearly unchanged, while the low-lying part at $E<12$ MeV becomes depleted significantly, worsening the agreement with the data. Increasing F_1 by around 20% restores the position of the GTR peak, but the depletion of the strength in the low-energy region remains. This shows the importance of pairing within the PDM in improving the agreement with the GTR distribution in the low-energy region. The effect of pairing on the GTR peak and its high-energy tail is not significant. This justifies the calculations without pairing within the PDM-2, as the computation here is rather complicated and takes much more CPU time. The results of the present work and [6] underpredict the data in the region of the high-lying tail ($E>30$ MeV). The experimental NEWSS, however, exceeds the GTR SR because of the contribution from the isovector-spin monopole resonance and the uncertainty involved in the multipole decomposition analysis used in extracting the data. This is clearly seen in Fig. 2, where the NEWSS in Eq. (5) are displayed as a function of excitation energy $E_{\max}$. The experimental NEWSS reaches the GTR SR at $E_{\max} \simeq 47$ MeV, and continues to increase at $E_{\max}>47$ MeV. The theoretical predictions approach the GTR SR at $E=70$ MeV. The values of the NEWSS, obtained in the region up to $E=22$ MeV, are 65.6% within the PDM-1, and 83% within the PDM-2 of GTR SR to be compared with the value 62.5% found in the experimental result in Fig. 2. The result within the PDM-1 agrees well with the experimentally extracted fraction of the GTR SR known as the quenched GTR. The PDM-2, however, predicts much less quenching for the GTR. In our understanding, an explicit inclusion of coupling to "$1p1h\otimes$ phonon" configurations, as is done within the PDM-2, restricts the flexibility in the adjustment of the parameter F_1, making it less effective compared to the PDM-1. Therefore, for a better quantitative prediction within the PDM-2, a realistic interaction is needed, which includes both short-range central as well as long-range tensor components.

In conclusion the PDM has been extended to the study of charge-exchange resonances. The results of numerical calculations of the GTR strength distribution are found to be in fair agreement with our previous calculations within an explicit microscopic approach [6] as well as the recent experimental data [8]. This shows the validity of the PDM in a qualitative description of GTR damping including its high-lying tail above 22 MeV. A better description for the strength distribution of GTR is obtained within the PDM-1 by using a more phenomenological parameter F_1, which effectively takes into account the contribution of coupling to complicated configurations. On the other hand, a smaller quenching obtained within the PDM-2 in the region below 22 MeV indicates that for a quantitative description of the spreading of GTR via an explicit coupling to "$1p_\pi 1h_\nu \otimes$phonon" configurations, a microscopic residual interaction such as those used in [4–6] must be employed.

[1] C. Gaarde, in *Proceedings of the Niels Bohr Centennial Conference on Nuclear Structure*, Copenhagen, 1985, edited by R. A. Broglia, G. B. Hagemann, and B. Herskind (Elsevier, Amsterdam, 1985), p. 449c.
[2] K. Shimizu, M. Ichimura, and A. Arima, Nucl. Phys. **A226**, 282 (1974).
[3] I. S. Towner and F. C. Khanna, Phys. Rev. Lett. **42**, 51 (1979).
[4] G. F. Bertsch and I. Hamamoto, Phys. Rev. C **26**, 1323 (1982).
[5] S. Drożdż, V. Klempt, J. Speth, and J. Wambach, Phys. Lett. **166B**, 18 (1986).
[6] N. Dinh Dang, A. Arima, T. Suzuki, and S. Yamaji, Phys. Rev. Lett. **79**, 1638 (1997); Nucl. Phys. **A621**, 719 (1997).
[7] M. Ericson, A. Figureau, and C. Thevenet, Phys. Lett. **45B**, 19 (1973); M. Rho, Nucl. Phys. **A231**, 493 (1974); E. Oset and M. Rho, Phys. Rev. Lett. **42**, 51 (1979).
[8] T. Wakasa *et al.*, Phys. Rev. C **55**, 2909 (1997).
[9] N. Dinh Dang and A. Arima, Nucl. Phys. **A636**, 427 (1998).
[10] N. Dinh Dang, K. Tanabe, and A. Arima, Phys. Rev. C **58**, 3374 (1998).
[11] N. Dinh Dang, V. Kim Au, and A. Arima, Phys. Rev. Lett. **85**, 1827 (2000).
[12] N. Dinh Dang, V. Kim Au, T. Suzuki, and A. Arima, Phys. Rev. C **63**, 044302 (2001).
[13] N. Van Giai and H. Sagawa, Nucl. Phys. **A371**, 1 (1981).